

## Semiconductor lasers for optical communication

A K SRIVASTAVA

Tata Institute of Fundamental Research, Homi Bhabha Road, Bombay 400 005, India

**Abstract.** Recent progress in the development of semiconductor lasers for optical-fibre communication is reviewed. GaInAsP buried heterostructure and distributed feedback structure, are described in some detail. An overview of the novel GaInAsSb mid-infrared (2–4 microns) lasers is also presented.

**Keywords.** Optical communication; semiconductor lasers; double heterostructure laser; buried heterostructure; distributed feedback structure.

### 1. Introduction

Recent years have seen considerable progress in the area of optoelectronic devices which are to be used in the optical fibre communication systems. State-of-the-art silica fibres have minimum dispersion and transmission loss (0.2 dB/km) at 1.3 and 1.55  $\mu\text{m}$  wavelength respectively (figure 1). Semiconductor emitters and detectors operating at these wavelengths are therefore very important. GaInAsP lasers having very low threshold currents for continuous wave (CW) operation at room temperature have been successfully developed for these wavelengths. More recently, optical fibres made of heavy-metal fluoride glasses are predicted to have transmission losses one to two orders of magnitude smaller than that of the best silica fibres. The minimum loss in these materials is expected to occur at the mid-infrared wavelengths (2–4  $\mu\text{m}$ ) (Lines 1984; Tran *et al* 1984). Optoelectronic materials and devices for these wavelengths are currently being investigated. GaInAsSb lasers for 2.2  $\mu\text{m}$  wavelength have been demonstrated recently. This review will focus on semiconductor lasers. After a brief introduction to the double heterostructure, some of the important laser structures like buried heterostructures (BH) and distributed feedback (DFB) structure, which have been realised using GaInAsP, will be described. Finally, recent progress in GaInAsSb lasers for mid-infrared wavelengths will be summarised.

### 2. GaInAsP lasers for 1.3 and 1.55 $\mu\text{m}$ wavelength

GaInAsP lasers are discussed in the following sections (Pearsall 1982; Agrawal and Dutta 1986).

#### 2.1 Double heterostructure (DH) laser

The basic structure of a *p-n* junction laser is shown in figure 2a. A pair of parallel planes are cleaved perpendicular to the plane of the junction. The two remaining sides of the diode are roughened to eliminate lasing in direction other than the main one. The structure is called a Fabry–Perot cavity. When a forward bias is applied to the laser diode, current flows and minority carriers are injected across the junction. Initially, at low currents, there is spontaneous emission in all

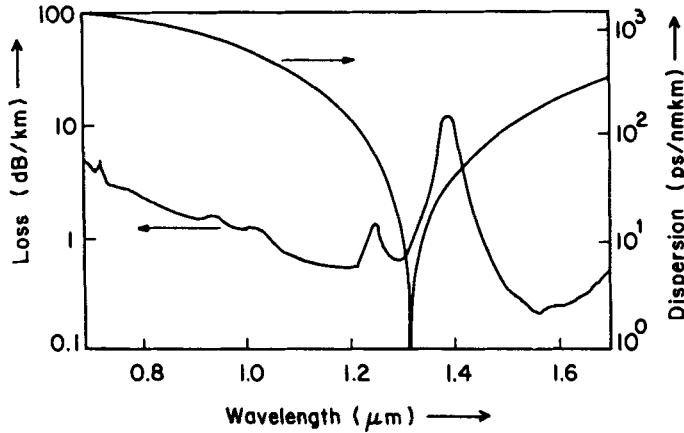


Figure 1. Attenuation and dispersion characteristics of a single mode silica fibre.

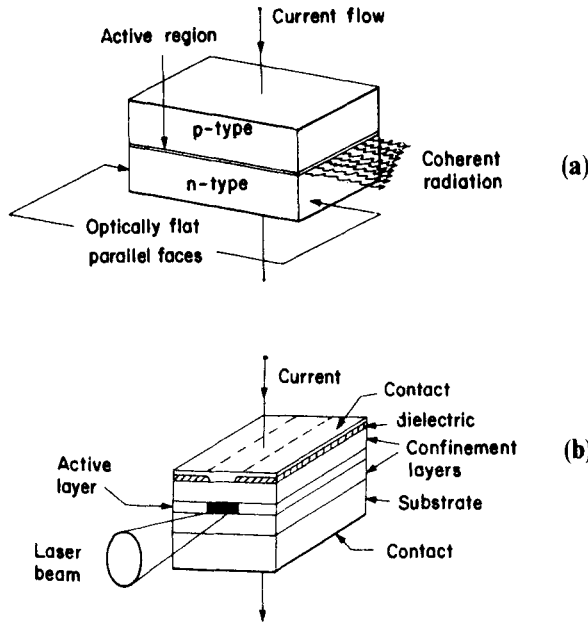


Figure 2. (a) Basic structure of a *p-n* junction laser in the form of a Fabry-Perot cavity. (b) Structure of a double heterostructure (DH) stripe laser.

directions. As the bias is increased, a threshold current is eventually reached when the optical gain in the structure is able to overcome the losses and stimulated emission occurs. A monochromatic and highly directional beam of light is emitted from the junction under these conditions. For the homostructure, the threshold current density  $J_{th}$  is very large ( $\approx 5 \times 10^4 \text{ A/cm}^2$ ) which makes it impossible to operate the laser continuously at room temperature.

To reduce the threshold current density, double heterostructure (DH) lasers have been proposed and built, using epitaxial techniques. Figure 2b shows the schematic

of a typical DH laser. The structure consists of an active layer sandwiched between two confining layers. All the layers are grown epitaxially and are lattice-matched to a suitable substrate. The confining layers are chosen to have higher bandgaps and lower refractive indices than that of the active layer at the operating wavelength. The  $p-n$  junction is incorporated at one of the heterojunctions by suitably adjusting the doping in the layers. When a forward bias is applied across the heterostructure, the injected carriers are confined within the active region by the heterojunction discontinuities. The optical field is also confined within the active region by the abrupt reduction in the refractive index outside the active region. These confinements enhance the stimulated emission and substantially reduce the threshold current density ( $\approx 10^3 \text{ A/cm}^2$ ). For 1.3 and 1.55  $\mu\text{m}$  lasers the active region and the confinement layers consist of quaternary GaInAsP alloy lattice-matched to an InP substrate (figure 3). The structures are generally grown by liquid phase epitaxy (LPE) or metal-organic chemical vapour deposition (MOCVD). The growth of the quaternary layers is rather critical as it is necessary to control the growth temperature to within a fraction of a degree in the region around 600°C. This is necessary for reproducible growth of a quaternary layer of given composition and thickness ( $\approx 0.1 \mu\text{m}$ ). The stripe structure shown in figure 2b usually gives multi-transverse modes. For efficient coupling of light to the fibre a single mode laser is required. This can be achieved by making mesa or ridge-type structures with 2-5  $\mu\text{m}$  wide ridges. One of the structures that has been successfully used to launch a large amount of power into a single mode fibre is the buried heterostructure.

## 2.2 Buried heterostructure laser

Figure 4 shows a schematic of the multiple-infil BH laser structure. The structure is

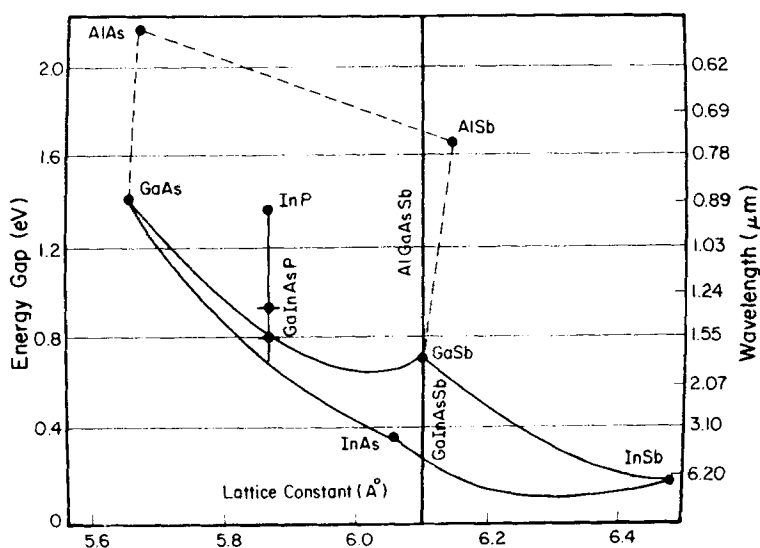


**Figure 3.** Variation of bandgap energy as a function of lattice-constant for III-V binary and alloy semiconductors.

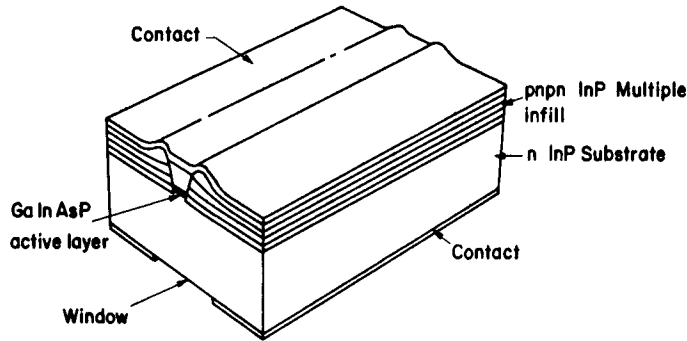
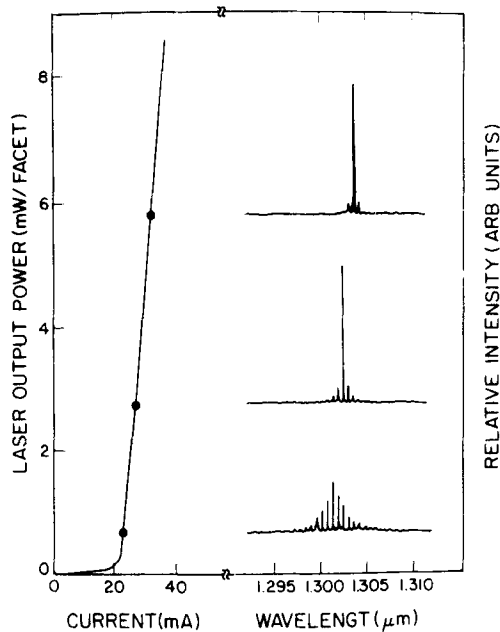


Figure 4. Schematic of a multiple infill buried heterostructure (BH) laser.

made using two successive epitaxial growth steps. First a DH structure of GaInAsP is grown on InP  $\langle 100 \rangle$  substrate. Next, a glassy masking layer is deposited onto the wafer and this is then photo-engraved leaving thin masking stripes running across the entire wafer surface. Careful preferential etching then follows which reveals the slow etching  $\langle 111 \rangle$  oriented planes of the ridge giving a reduced width of the waist ( $\approx 1 \mu\text{m}$ ) below the top of the ridge. The active quaternary layer is arranged to be close to the "waist" of the ridge. The wafer then goes through a second epitaxial growth stage in which a series of *p*-type, intrinsic and *n*-type layers (or one thick semi-insulating layer) of InP are deposited. These layers stack up the sides of the ridge to produce a structure with cross-section as shown in figure 4. Thus the quaternary active layer is cladded above, below and on the sides by layers of lower refractive index and we have full optical confinement in the vertical and lateral planes. The multilayers on either side of the active layer incorporate several reverse biased *p-i-n* junctions (or the semi-insulating layer) which effectively block the current spreading and thereby reduce threshold current. These structures have threshold currents in the range 10–20 mA. The light-current characteristics of a  $1.3 \mu\text{m}$  BH laser is shown in figure 5. These lasers can typically provide 10–20 mW of power output per facet. The spectrum of a  $1.3 \mu\text{m}$  BH laser is also shown in the figure. As mentioned earlier, the laser wave-guide is designed to support only one transverse mode in the vertical plane. In the horizontal plane, although in principle several modes could propagate, scattering at the mesa edges preferentially attenuates higher order modes and again limits operation to only one mode. The spectrum therefore indicates single transverse mode with several longitudinal Fabry–Perot modes separated by  $\approx 10 \text{ \AA}$ . The frequency response of BH lasers shows resonance at  $\approx 10 \text{ GHz}$  implying a pulse modulation capability of these lasers in the Gbit/s region. The spectral linewidth of BH lasers is however rather large (2–5  $\text{ \AA}$ ) which makes it unsuitable for long haul communication systems. Of the several schemes employed to reduce the spectral width, the most successful one has been the distributed feedback (DFB) structure.

### 2.3 Distributed feedback (DFB) structure

The Fabry–Perot cavity consisting of two parallel cleaved facets in the semiconductor lasers gives rise to several longitudinal modes spread over the gain



**Figure 5.** Light output vs current curve for a  $1.3 \mu\text{m}$  buried heterostructure laser. Optical power spectra for three different power output levels are also indicated in the figure.

curve of the laser (figure 5). These modes seriously limit the distance over which communication can be made on the optical fibre due to chromatic dispersion. Ideally one would like to have a single mode very narrow spectral-width laser for such applications. Reducing the laser length increases the spacing of the Fabry-Perot modes and is a possible solution but it increases the lasing threshold, makes fabrication more difficult (typically lasers are  $250 \mu\text{m}$  long) and makes it necessary to use high reflection coatings on the laser facets. Figure 6a shows the schematic of a DFB laser which overcomes this problem. The structure is made by etching a fundamental or second order grating of period  $0.2$  to  $0.4 \mu\text{m}$  in the material before growth of the DH structure. As shown in figure 6b an optical wave travelling across the active region is partially reflected at the peaks and valleys of the grating because of the change in the effective refractive index sampled by the wave. Only that wavelength for which this feedback interferes constructively is amplified and the rest are suppressed. Spectral characteristics of DFB GaInAsP lasers show reduction in the spectral width ( $\approx 0.1 \text{ \AA}$ ) and nearly total suppression of side bands. In addition, the incorporation of the grating makes the emission wavelength almost independent of temperature. These advantages of DFB lasers make them suitable for long distance communication systems.

### 3. GaInAsSb lasers for $2\text{--}4 \mu\text{m}$ wavelength

Figure 7 shows the layer structure of a GaInAsSb/AlGaAsSb DH laser. The layers of the quaternary alloys GaInAsSb and AlGaAsSb are epitaxially grown on GaSb substrate. In figure 3 the position of these alloys has been marked on a bandgap

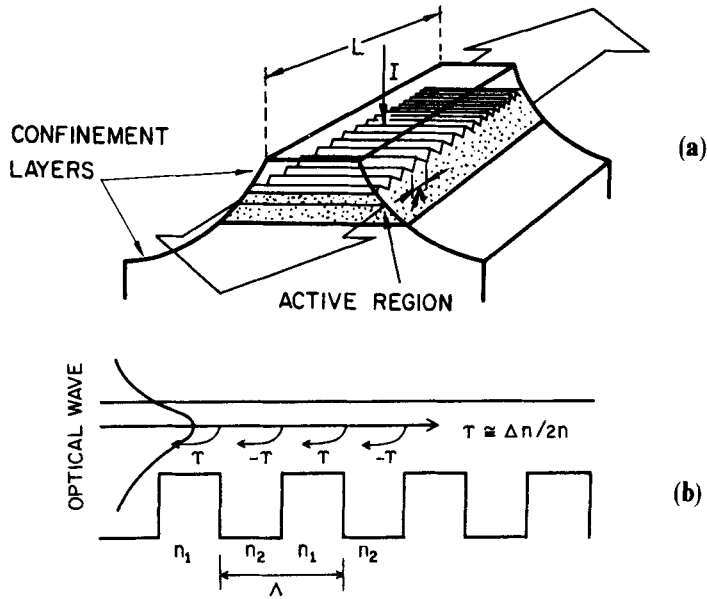


**Figure 6.** (a) Schematic of a distributed feedback (DFB) laser. (b) Mechanism of wavelength selection by grating in a DFB laser. Constructive interference takes place for wavelength  $\lambda$  satisfying  $(2\pi/\lambda)n\Lambda + \pi = 2\pi$ .

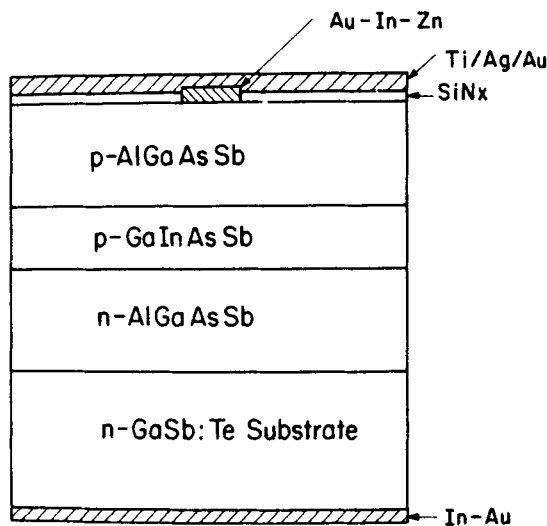


**Figure 7.** Schematic of the cross-section of a GaInAsSb/AlGaAsSb DH laser.

energy vs lattice-constant diagram. As indicated in the figure, the composition of the GaInAsSb active layer isoperiodic with GaSb can be adjusted to vary the laser emission wavelength between 1.7 and 4.3  $\mu\text{m}$ . Also indicated in the figure is the position of AlGaAsSb alloy, lattice-matched to GaSb, which with its higher bandgap energy and lower refractive index serves as a suitable confinement layer material.

Several crystal growth techniques (LPE, MOCVD and MBE) have been employed to grow GaInAsSb on a GaSb substrate. However, the best results have been obtained by LPE (DeWinter *et al* 1985). DH lasers have been successfully grown by LPE on *n*-type,  $\langle 100 \rangle$  oriented GaSb substrates in a conventional horizontal-slider/graphite boat apparatus at 530°C (Caneau *et al* 1985). Early work on GaInAsSb/AlGaAsSb DH lasers resulted in room temperature, pulsed  $J_{th}$  values of 5 kA/cm<sup>2</sup> at 1.8  $\mu\text{m}$  wavelength (Kobayashi *et al* 1980) and CW operation of 2.0  $\mu\text{m}$  lasers only at 80 K (Kano and Sugiyama 1980). Room temperature lasers for longer wavelengths have been reported with  $J_{th}$  values of 14 kA/cm<sup>2</sup> at 2.02  $\mu\text{m}$  and 20 kA/cm<sup>2</sup> at 2.29  $\mu\text{m}$  (Bochkarev *et al* 1985).

Recently, pulsed room temperature 2.2 microns lasers with  $J_{th}$  values as low as 3.5 kA/cm<sup>2</sup> have been reported (Caneau *et al* 1986a). These lasers operated CW up to 235 K temperature (Caneau *et al* 1987). The laser structure used in this work consisted of an active layer of Ga<sub>0.84</sub>In<sub>0.16</sub>As<sub>0.15</sub>Sb<sub>0.85</sub> between two Al<sub>x</sub>Ga<sub>1-x</sub>As<sub>y</sub>Sb<sub>1-y</sub> confinement layers, lattice-matched to GaSb substrate. Two compositions for the confinement layers were used: for one type of structure (DH-I),  $x=0.27$  and  $y=0.04$ , and for the other (DH-II),  $x=0.34$  and  $y=0.04$ . Figure 8 shows the light output vs current ( $L-I$ ) curve of a DH-I laser with 1  $\mu\text{m}$  thick active layer. The inset shows a low-resolution spectrum of the laser output with a peak wavelength of 2.2  $\mu\text{m}$ . For DH-I lasers the lowest  $J_{th}$  value was 6.9 kA/cm<sup>2</sup> and this occurred for an active layer thickness ( $d$ ) of 0.8 to 1.0  $\mu\text{m}$ , while for DH-II lasers, the optimal thickness was found to be 0.5  $\mu\text{m}$  and resulted in  $J_{th}$  value of 3.5 kA/cm<sup>2</sup>. The lower  $J_{th}$  and smaller optimum  $d$  values for DH-II lasers as compared to DH-I lasers result primarily from improved optical confinement by more Al-rich confinement layers. Further reduction in  $J_{th}$  value (1.7 kA/cm<sup>2</sup>) for these lasers has been recently reported (Caneau *et al* 1987). Figure 9 shows the  $L-I$  curves for DH-II lasers operated under CW conditions at various temperatures. CW operation was achieved up to 220 K with a threshold current of 125 mA. The same laser mounted with improved soldering for more effective heat sinking operated CW at temperatures up to 235 K. The characteristic temperature  $T_0$  was measured to be 55 K and 80 K for DH-I and DH-II lasers respectively. More recently (Joullie *et al* 1988),  $T_0$  has been reported to be 90 K for these lasers. Figure 10 shows the

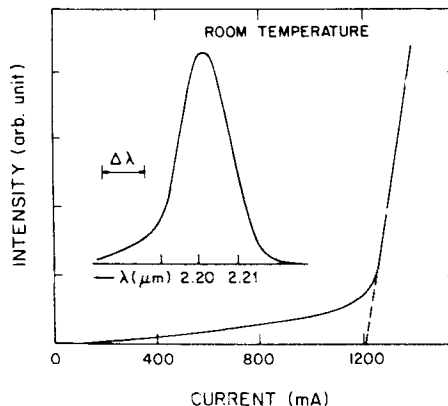


**Figure 8.** Light intensity vs current characteristics of a GaInAsSb DH laser. Spectrum shown in the inset peaks at 2.2  $\mu\text{m}$ ; the monochromator resolution,  $\Delta\lambda$ , is 0.01  $\mu\text{m}$ .

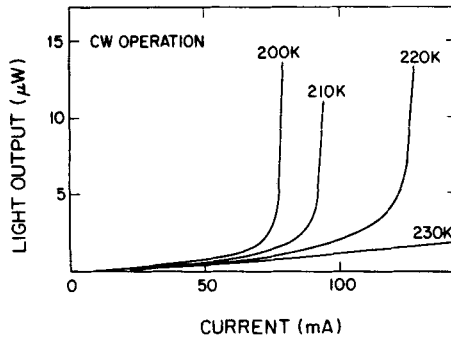


Figure 9. CW light output vs current curves for a DH-II laser at different temperatures.

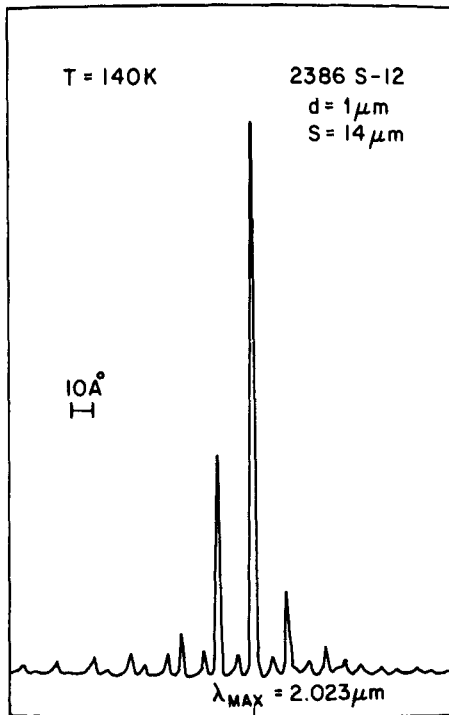


Figure 10. Emission spectrum of a GaInAsSb stripe laser operated under quasi-CW conditions at 140 K.

spectrum of a GaInAsSb laser (Caneau *et al* 1986b) at 140 K. The device was operated under quasi-CW condition with long current pulses. Two sets of Fabry-Perot modes are visible, corresponding to the excitation of the first order in addition to the fundamental transverse mode.

#### 4. Summary

Considerable progress has been made in the development of semiconductor lasers

for optical-fibre communication. GaInAsP lasers emitting at 1.3 and 1.55  $\mu\text{m}$  wavelength are advanced sufficiently to be included in communication systems. Mid-infrared GaInAsSb semiconductor lasers with room temperature threshold current densities as low as 1.7 kA/cm<sup>2</sup> and capable of CW operation at temperatures up to 235 K have been demonstrated. At room temperature these lasers emit at 2.2  $\mu\text{m}$  wavelength. The present results show the promise of these lasers for future ultra-low-loss mid-infrared communication systems.

## References

- Agrawal G P and Dutta N K 1986 in *Long wavelength semiconductor lasers* (New York: Van Nostrand Reinhold)
- Bochkarev A E, Dolginov L M, Drakin A E, Druzhinina L V, Eliseev P G and Sverdlov B N 1985 *Sov. J. Quantum Electron.* **15** 86
- Caneau C, Srivastava A K, Dentai A G, Zyskind J L, Burrus C A and Pollack M A 1986a *Electron. Lett.* **22** 992
- Caneau C, Srivastava A K, Dentai A G, Zyskind J L and Pollack M A 1985 *Electron. Lett.* **21** 815
- Caneau C, Srivastava A K, Zyskind J L, Sulhoff J W, Dentai A G and Pollack M A 1986b *Appl. Phys. Lett.* **49** 55
- Caneau C, Zyskind J L, Sulhoff J W, Glover T E, Centanni J, Burrus C A, Dentai A G and Pollack M A 1987 *Appl. Phys. Lett.* **51** 764
- DeWinter J C, Pollack M A, Srivastava A K and Zyskind J L 1985 *J. Electron. Mater.* **14** 729
- Joullie A, Alibert C, Mani H, Pitard F, Tournie E and Boissier G 1988 *Electron. Lett.* **24** 1076
- Kano H and Sugiyama K 1980 *Electron. Lett.* **16** 146
- Kobayashi N, Horikoshi Y and Uemura C 1980 *Jpn. J. Appl. Phys.* **19** L30
- Lines M E 1984 *Science* **226** 663
- Pearsall T P 1982 *GaInAsP alloy semiconductors* (New York: John Wiley & Sons)
- Tran D C, Sigel G H Jr and Bendow B 1984 *J. Lightwave Technol.* **LT-2** 566